Eur. Phys. J. D **21**, 153–161 (2002)
DOI: 10.1140/epjd/e2002-00201-5

THE EUROPEAN PHYSICAL JOURNAL D

Spectroscopy of calcium deposited on large argon clusters

M.A. Gaveau[1], M. Briant[1], P.R. Fournier[1], J.M. Mestdagh[1,a], J.P. Visticot[1], F. Calvo[2], S. Baudrand[2], and F. Spiegelman[2]

[1] Laboratoire Francis Perrin[b], CEA Saclay, 91191 Gif-sur-Yvette Cedex, France
[2] Laboratoire de Physique Quantique[c], IRSAMC, Université Paul Sabatier, 118 route de Narbonne, 31062 Toulouse Cedex, France

Received 7 May 2002
Published online 1st October 2002 –

Abstract. Spectroscopic experiments have been performed, providing emission and excitation spectra of calcium atoms trapped on argon clusters of average size 2 000. The two experimental spectra fall in the vicinity of the calcium resonance line $^1P_1 \rightarrow {}^1S_0$ at 422.9 nm. The excitation spectrum consists in two bands located on each side of the resonance line of the free calcium. In addition, Monte Carlo calculations, coupled to Diatomics-In-Molecule potentials are employed to simulate the absorption spectrum of a single calcium atom in the environment of a large argon cluster of average size 300. The theoretical absorption spectrum confirms the existence of two bands, and shows that these bands are characteristic of a calcium atom located at the surface of the argon cluster and correspond to the excited $4p$ orbital of calcium either perpendicular or parallel to the cluster surface. The precise comparison between the shape of the absorption spectrum and that of the fluorescence excitation spectrum shows different intensity ratios. This could suggest the existence of a non adiabatic energy transfer that quenches partly the fluorescence of trapped calcium. Another explanation, although less likely, could be a substantial dependence of the calcium oscillator strength according to the alignment of the calcium excited orbital with respect to the cluster surface. The emission spectrum always shows a band in the red of the resonance line which is assigned to the emission of calcium remaining trapped on the cluster. When exciting the blue band of the excitation spectrum, the emission spectrum shows a second, weak, component that is assigned to calcium atoms ejected from the argon clusters, indicating a competition between ejection and solvation.

PACS. 36.40.-c Atomic and molecular clusters – 82.33.Hk Reactions on clusters

1 Introduction

Recent work has focused the attention on the dynamics of reactants deposited on large rare gas clusters, leading to studies of *Cluster Isolated Chemical Reactions* (CICR) [1–3]. The aim is to give a microscopic information on the effect of a condensed reaction medium on chemical reactions. In such studies, the reaction environment is modelled by large van der Waals clusters (a few hundred to a few thousand atoms) in a molecular beam on which the reactants are deposited by pick-up.

Several groups are active in this field, and various processes have been documented in the environment of a rare gas cluster: association reaction between two reactants [4], photodissociation of HBr [5–7], chemiluminescence in the bimolecular $Ba + N_2O \rightarrow BaO^* + N_2$ reaction within either argon, neon [8] or helium clusters[9], transition state spectroscopy of the I+HI reaction by photodetachment in $IHI^-(Ar)_n$ clusters [10]. Very recently, the $Ca^* + HBr \rightarrow CaBr^* + H$ reaction has been photoinduced starting from the $Ca\cdots HBr$ complex that is deposited at the surface of a large argon cluster. The corresponding dynamics has been investigated thoroughly [11]. Clearly, such studies benefit of a good knowledge of the interaction between the reactants and the cluster environment. This was exemplified by the work on the HBr photodissociation which involved both experimental measurements [5,7] and theoretical investigations of the HBr-cluster interaction [6].

The interaction of a single calcium atom with a rare gas cluster, helium, has been address by Stienkemeier and coworkers [12]. The present work is both experimental and theoretical. It investigates the situation where a single calcium atom interacts with an argon cluster. Experimentally, this has been achieved by conducting laser induced fluorescence in the vicinity of the calcium resonance line at 422.9 nm. This provides us with both fluorescence spectra of calcium and excitation spectra of this fluorescence, which reflect the interaction of calcium with its environment. In parallel, a DIM (Diatomic-In-Molecule) model

[a] e-mail: jmm@drecam.saclay.cea.fr
[b] URA 2453 du CNRS
[c] UMR 5626 du CNRS

and a Monte Carlo sampling are used in tandem to simulate the absorption spectrum of calcium. Comparison of this spectrum with the experimental fluorescence excitation spectrum is expected to bring the information whether calcium is solvated partially and stays at the cluster surface, or is fully solvated and embedded inside the cluster. Such information is of particular importance in CICR experiments since the location of the reactants drastically affects the initial conditions of the reaction. The other information that is expected by the comparison between experiment and theory is dynamical, indicating whether non adiabatic processes enter into play for quenching the calcium fluorescence. A distinction must be made indeed at this point between the excitation spectrum of the calcium fluorescence and the absorption spectrum. Both spectra are equivalent when no process is present to quench the electronic excitation. However, in the present case, since calcium is in interaction with an argon cluster, non adiabatic energy transfer toward dark states may exist, and the comparison between both types of spectra could be informative regarding this issue.

A work in that direction was already achieved in our laboratory for a single barium atom interacting with an argon cluster [13,14]. Surface location of barium was found. Unfortunately, the complete interpretation of the experimental spectra, which involves the coupling between DIM potentials and molecular dynamics calculations, was difficult because no reliable potential energy curve was available on the Ba*–Ar system that could be used in the DIM calculation to simulate accurately the Ba*-argon cluster interaction. In a recent work, a complete set of accurate potential energy curves describing the interaction of the ground state and excited states of calcium with argon, up to the doubly excited configuration $4p^2$ has been calculated [15]. These curves enable the construction of a consistently based DIM model. This model is coupled to a Monte Carlo simulation that can deal with larger cluster sizes than the molecular dynamics calculations of the earlier work on the $Ba(Ar)_n$ system.

The experimental setup and the experimental technique are described in Section 2. The DIM model and the Monte Carlo simulation technique are presented in Section 3. Both the experimental and the theoretical results are presented and discussed in Section 4.

2 Experimental details

The experimental apparatus is fully described in references [8,16,17]. Briefly, argon clusters of average size 2 000 are generated from a 20 bars continuous supersonic expansion through a 0.2 mm sonic nozzle at room temperature in a Campargue molecular beam source [18]. After double extraction by a 1 mm skimmer and a 3 mm collimator, the cluster beam enters into the main chamber of the experimental setup where the clusters undergo deposition of calcium atoms by the well established pick-up technique [19,20]. At 17 mm downstream from the exit of the pick-up cell, the cluster beam reaches the laser excitation region, which is illuminated by the light of an extra-cavity doubler Wavetrain pumped by a cw tunable single frequency Ti:sapphire laser (Coherent 899-21). The doubled wavelength can be adjusted from 391 to 432 nm in the vicinity of the calcium resonance line ($^1P_1 \rightarrow {}^1S_0$) at 422.9 nm. The laser light is a slightly converging vertical beam, perpendicular to the cluster beam. Optics allows us to collected fluorescence light emitted in the excitation region. About 90% of the collected fluorescence light is focused on the entrance slit of a scanning grating monochromator. The other 10% are undispersed and sent on a second photomultiplier in order to monitor the total fluorescence.

Two types of spectra were recorded, (i) emission spectra, by exciting calcium at a fixed wavelength of the laser and scanning the monochromator wavelength; (ii) excitation spectra, by varying the laser frequency and measuring either the total fluorescence or the fluorescence at a fixed monochromator wavelength.

In order to eliminate non relevant contributions in the emission spectra, such as blackbody radiation from the pick-up cell and fluorescence of free calcium effusing from the pick-up cell, the cluster beam is flagged alternatively on and off prior to the pick-up cell. The resulting two spectra are subtracted from each other, hence providing the specific emission due to calcium deposited on clusters.

In practice, it is impossible to sweep the laser frequency continuously, because the extra-cavity doubler has to be readjusted when changing the wavelength of the titane-sapphire laser. Hence, the excitation spectrum is recorded step by step. At each step, the laser is tuned at the desired wavelength and the corresponding emission spectrum is stored. The excitation spectrum is constructed from these emission spectra by integrating each of them and normalizing the integral according to the laser power.

3 Model and simulations

The present theoretical approach simulates the absorption spectrum of calcium deposited on an argon cluster. The simulation is performed in the following way. A Monte Carlo sampling of acceptable ground state geometries of the calcium atom within the argon cluster is performed. For each of these geometries, the strength and the wavelength of the transition between singlet ground state calcium ($4s^2$ configuration) and the singly excited states corresponding to the $4s4p$ configuration are calculated. The histogram of the oscillator strengths is accumulated as a function of the excitation energies. This histogram simulates the absorption spectrum of calcium in the cluster environment.

3.1 The DIM model

A quantum Hamiltonian based on the Diatomics-In-Molecules approximation has been developed to describe the interaction between the argon cluster and the states

of a Ca atom belonging to the $4s^2$ and $4s4p$ configurations. Similar DIM models have been previously used for alkali [21,22] or alkaline-earth [14,23] atoms.

The ground state $4s^2\ ^1\mathrm{S}_0$ of calcium is described as a single determinant $\Phi_0 = |4s\bar{4s}|$. In the following, its potential energy surface (PES) is taken as a sum of Ca–Ar (V_0) and Ar–Ar (V_{ArAr}) pairwise potentials given below. The excited states corresponding to the $4s4p$ configuration can be obtained from this reference determinant as

$$\Phi_{\mu\zeta\chi} = a^\dagger_{\mu\zeta} a_{s\chi} \Phi_0, \tag{1}$$

where $\mu = (x, y, z)$ labels the spatial orientation of the excited electron. ζ and χ label the spin projections. $a^\dagger_{\mu\zeta}$ is the creation operator of an electron in orbital $4p_\mu$ with spin projection ζ, and $a_{s\chi}$ is the annihilation operator of an electron in orbital $4s$ with spin projection χ. In order to compute the DIM Hamiltonian of a Ca atom interacting with a set of argon atoms labelled $i = 1 \ldots N$, one defines orbitals μ in the fixed frame, and also a set of local functions λ that are either parallel ($\lambda = \sigma$) or perpendicular ($\lambda = \pi_x, \pi_y$) to each Ca–Ar-axis. The rotation matrices $\rho^i_{\lambda\mu}$ map the local basis λ onto the fixed basis μ for each atom i. The nonzero matrix elements of the DIM matrix can be written as

$$\begin{aligned} H_{\mu\zeta\chi,\mu'\zeta\chi} &= e_0\delta_{\mu\mu'} + \sum_{i=1}^{N}\sum_{\lambda=1}^{3} \rho^i_{\lambda\mu}\rho^i_{\lambda\mu'}\left[V_\lambda(r_i) - K_\lambda(r_i)\delta_{\zeta\chi}\right] \\ H_{\mu\zeta\chi,\mu'\chi\zeta} &= \sum_{i=1}^{N}\sum_{\lambda=1}^{3} \rho^i_{\lambda\mu}\rho^i_{\lambda\mu'} K_\lambda(r_i). \end{aligned} \tag{2}$$

In the equations above, $e_0 = 0.572893$ is the average atomic transition energy of calcium [15]:

$$e_0 = \frac{1}{2}\left[E(4s4p\ ^1\mathrm{P}) + E(4s4p\ ^3\mathrm{P})\right] - E(4s^2\ ^1\mathrm{S}). \tag{3}$$

r_i is the distance between Ca and the ith argon atom; $V_\lambda(r)$ is the spin-independent potential energy of a CaAr excited determinant (with symmetry Σ or Π). $K_\lambda(r)$ is a distance-dependent exchange integral $\langle s(1)\lambda(2)|1/r_{12}|\lambda(1)s(2)\rangle$, which tends to the atomic exchange integral asymptotically $K_\lambda(\infty) = 0.018242$ a.u. Again, $K_\lambda(\infty)$ is obtained from the atomic levels [15]:

$$K_\lambda(\infty) = \frac{1}{2}\left[E(4s4p\ ^1\mathrm{P}) - E(4s4p\ ^3\mathrm{P})\right]. \tag{4}$$

The interactions V_λ and K_λ were taken from a pseudopotential calculation of the CaAr diatomic molecule [15]. At this step, the eigenvalues and eigenvectors of the DIM Hamiltonian represent the adiabatic potential energy surface of the system (neglecting spin-orbit coupling). Indeed, for any given distance between the Ca and Ar atoms, the relationship between V_λ, K_λ, and the energies of the $4s4p$ states reduces to ${}^{3,1}E_\lambda = V_\lambda \pm K_\lambda$. Thus the functions V_λ and K_λ can be readily obtained from the ${}^{3,1}\Pi$ and ${}^{3,1}\Sigma$ potential energy curves of CaAr.

Table 1. Parameters of the DIM functions (5, 6), given in atomic units. Undefined coefficients are zero.

	V_0	V_π	V_σ	K_π	K_σ
A	14.6732	11.3335	6.50		
γ	1.09357	1.16799	0.835934		
C_4				35.3725	156.523
C_5				−1084.62	−8573.6
C_6	−606.872	−396.412	−1488.39	11479.8	173506.0
C_7				−49900.7	-1.60348×10^6
C_8				76616.2	6.14742×10^6
C_{10}					-4.75009×10^7
C_{12}	6.4×10^5	9585.0	3.34501×10^6		2.5477×10^8

The functions V (V_π, V_σ, and the ground state V_0) were fitted according to a simple exp-6-12 expression:

$$V(r) = A\exp(-\gamma r) + \frac{C_6}{r^6} + \frac{C_{12}}{r^{12}}\cdot \tag{5}$$

The functions K_π and K_σ were taken as rational fractions of r:

$$K(r) = K(\infty) + \sum_{n=4}^{12}\frac{C_n}{r^n}\cdot \tag{6}$$

The parameters are given in Table 1. Finally, the Ar–Ar interaction $V_{\mathrm{ArAr}}(r)$ is modelled by a simple Lennard-Jones potential $4\varepsilon[(\sigma/r)^{12} - (\sigma/r)^6]$ with $\varepsilon = 4.5935 \times 10^{-4}$ Hartree and $\sigma = 6.236$ bohr, which corresponds to $R_e = 7.0$ bohr.

Spin-orbit (SO) coupling of the calcium atom has been included in the present calculation. The Atom-In-Molecule (AIM) scheme of Cohen and Schneider [24] has been used for the $4s4p$ configuration, using $\zeta_{4p} = 105.9\ \mathrm{cm}^{-1}$ [25]. The Hamiltonian (2) is supplemented with the following one-electron SO operator

$$H_{\mathrm{SO}} = \zeta_{4p} \sum_{j}^{\text{electrons}} \hat{\ell}_j \cdot \hat{s}_j. \tag{7}$$

The diagonalization of the 12×12 resulting matrix $H + H_{\mathrm{SO}}$ yields the excited DIM eigenstates Ψ_m and eigenvalues E_m including SO coupling:

$$\Psi_m = \sum_{\mu\zeta\chi} c^m_{\mu\zeta\chi}\Phi_{\mu\zeta\chi}. \tag{8}$$

Apparently, the mixing of triplet and singlet states remains extremely weak and the absorption of the upper singlet states is several orders of magnitude larger than that of triplet states.

As a final step in the calculation, the dipole moments between the ground state Φ_0 and the excited states Ψ_m were also approximated in an AIM scheme as

$$D^\nu_{0m} = \langle\Phi_0|\nu|\Psi_m\rangle = d_{\mathrm{sp}}(c^m_{\nu\alpha\alpha} + c^m_{\nu\beta\beta}), \tag{9}$$

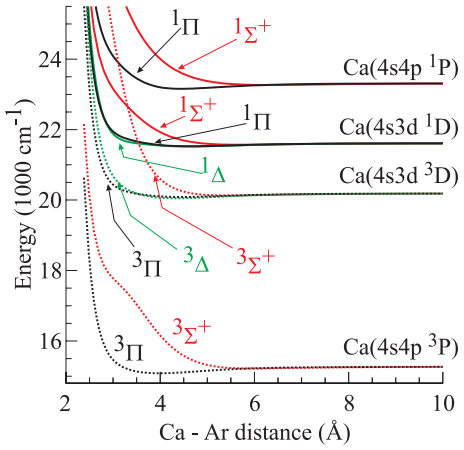

Fig. 1. Potential energy curves of CaAr dissociating into the $4s4p$ and $4s3d$ atomic configurations. Taken from reference [15].

where $\nu = x$, y, z, and α, β the eigenstates of the spin projections. $d_{\rm sp}$ is the atomic one-electron integral $\langle 4s(1)|x|4p(1)\rangle$.

The low lying curves of the CaAr molecule are shown in Figure 1. The relevant curves for the present calculation are those correlating with the $4s4p$ ^{1}P and $4s4p$ ^{3}P states of calcium.

A crossing is observed in Figure 1 between the $^3\Sigma$ curve correlating with Ca($4s3d$ ^{3}D)+Ar and the $^1\Pi$ curve correlating with Ca($4s4p$ ^{1}P)+Ar. This results on CaAr into a vanishing coupling between the two curves, as far as SO coupling is not considered, and certainly very weak, even when it is included. Nevertheless, it is likely to induce a non adiabatic energy transfer. In clusters, the position of such crossings will vary, however it will remain as a singlet-triplet interaction. Despite this expected weak interaction, one cannot exclude that the $4s3d$ states, not included in the present model, may cause fluorescence quenching. Such a process is one of those anticipated in the introduction, by which the absorption spectrum of calcium in the Ca(Ar)$_n$ system may differ from the excitation spectrum of the calcium fluorescence. Except in its close vicinity, the crossing does not affect the shape of the absorption spectrum and the $4s3d$ configuration does not need to be included in the DIM model.

3.2 Monte Carlo simulations

The above DIM model is associated to a Monte Carlo simulation in the same way as described in reference [26]. A random walk on the ground state PES $E_0(\mathbf{R})$ is performed at a temperature of 35 K corresponding to that known experimentally for argon clusters [27]. Sampling of relevant configurations is used to accumulate the vertical absorption spectrum along the trajectory, as well as structural quantities such as the radial density of argon atoms around calcium. The absorption spectrum at energy ε corresponds to the Boltzmann-weighted intensity for each configuration:

$$\mathcal{I}(\varepsilon) = \frac{8\pi^2}{3} \times \frac{\int \sum_m \varepsilon_{0m}(\mathbf{R}) |D_{0m}|^2 \delta[\varepsilon - \varepsilon_{0m}(\mathbf{R})] \exp\left[\frac{-E_0(\mathbf{R})}{k_{\rm B}T}\right] {\rm d}\mathbf{R}}{\int \exp\left[\frac{-E_0(\mathbf{R})}{k_{\rm B}T}\right] {\rm d}\mathbf{R}}. \quad (10)$$

In this equation we have denoted $\varepsilon_{0m} = E_m - E_0$ the transition energy between the ground state and excited state Ψ_m.

Although the MC simulation is quite efficient, the calculation could not be run on Ar$_{n\approx 2\,000}$ clusters as those present in the experiment. The calculation has been carried out for a smaller size of 300, using 2.5×10^5 Monte Carlo cycles (1 cycle $= n + 1$ steps), of which the first 5×10^4 were discarded for equilibration. To mimic the broad log-normal size distribution of the clusters in the beam, calculations have been performed also at sizes 200 and 400. The three calculations have been averaged with the respective weights 50%, 25% and 25%.

4 Results and discussion

4.1 Fluorescence spectra

We first present the experimental results concerning the calcium fluorescence. Figure 2 displays two emission spectra of the Ca(Ar)$_n$ with $\bar{n} \approx 2\,000$ system that have been recorded with a resolution of 0.5 nm at two laser wavelengths located on both sides of the calcium resonance line. The reason for choosing these two wavelengths will appear in the next section. In the bottom panel of Figure 2, the excitation wavelength is on the red side of the Ca resonance line at 425.9 nm (23 480 cm^{-1}). The spectrum consists in a single band peaking at 23 300 cm^{-1} (429 nm) with a FWHM of $\approx$ 150 cm^{-1}. The emission spectrum displayed on the top panel of Figure 2 has been recorded for an excitation wavelength of 411.2 nm (24 319 cm^{-1}), *i.e.* in the blue wing of the calcium resonance line. It presents two components: a band similar to that of the bottom panel spectrum, plus the calcium resonance line at 422.9 nm (23 652 cm^{-1}), the position of which is indicated by the vertical dashed line.

These spectra are qualitatively similar to those found in our former works on the Ba(Ar)$_n$ systems [14,28]. Hence, the qualitative interpretation given in these latter works may apply here with calcium. The broad emission located to the red side of the resonance line of free calcium is assigned to calcium atoms that stay solvated within the argon cluster until they emit light. When exciting the Ca(Ar)$_{\overline{n}\approx 2\,000}$ system to the red side of the resonance line of free calcium, there is not enough energy in the system for calcium to simultaneously leave the cluster and stay electronically excited. Hence, only the broad

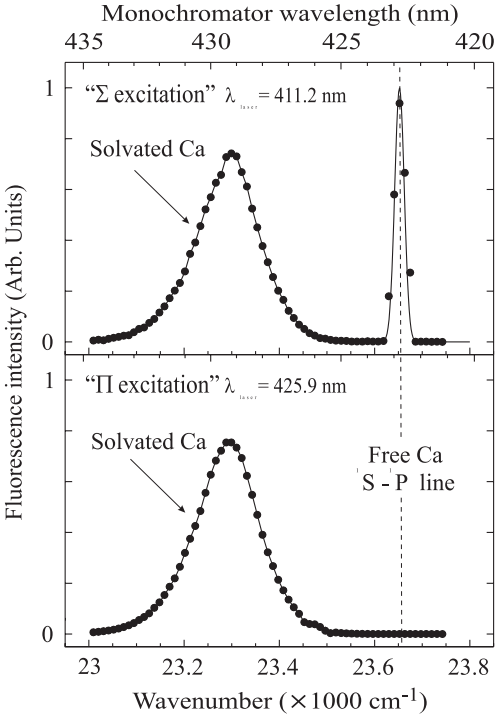

Fig. 2. Emission spectra after excitation of the $Ca(Ar)_{n\approx 2\,000}$ system at either 411.2 nm (top panel) or 425.9 nm (bottom panel). The solid line passing through the experimental point is simply for guiding the eyes.

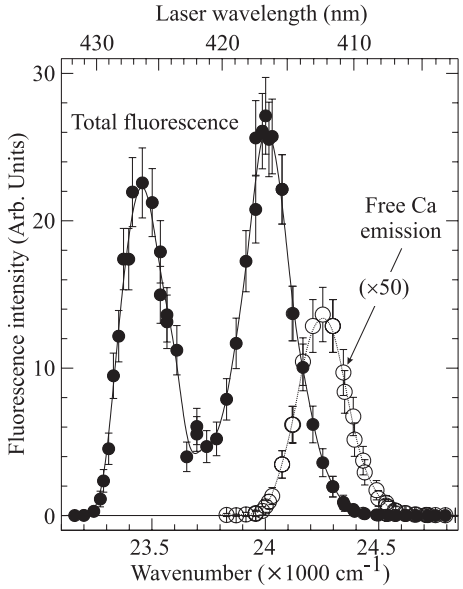

Fig. 3. Excitation spectra of the $Ca(Ar)_{n\approx 2\,000}$ system. The filled symbols and solid line corresponds to exciting the total fluorescence. The open symbols and dashed line shows, after multiplication by a factor 50, the spectrum corresponding to excitation of atoms that emits as free $Ca(4s4p\ ^1P)$.

emission due to solvated calcium is observed. On the contrary, when calcium is excited to the blue wing of the resonance line, enough energy is available for calcium to leave the cluster, still being electronically excited. In that case, emission from free calcium is expected. The top spectrum in Figure 2 shows that emission of both free and solvated calcium is observed, a dynamical indication that ejection of calcium is in competition with solvation.

4.2 Excitation spectra of the calcium fluorescence

Considering that upon excitation of $Ca(Ar)_{n\approx 2\,000}$, calcium emits both as solvated and as free atom, two excitation spectra need to be measured experimentally. The excitation spectrum of $Ca(Ar)_{n\approx 2\,000}$ corresponding to emission of free calcium is shown after multiplication by a factor 50 as a dashed line running through the experimental points in Figure 3.

The excitation spectrum for the emission of free calcium is exclusively located in the blue wing of the full excitation spectrum. This makes sense considering the energetic argument given in the previous section. This further indicates that ejection of calcium is significant only when enough energy is deposited in the system. The ejection process of an alkaline earth atom (barium) out of an argon cluster has been examined in detail in a former work [28] and does not need to be commented further.

The excitation spectrum of the total fluorescence has two components of approximately 250 cm^{-1} width located on both sides of the Ca resonance line (422.9 nm, 23 652 cm^{-1}): (i) the first one, with a maximum at 416.6 nm (24 000 cm^{-1}) is shifted by about 350 cm^{-1} to the blue side of the Ca resonance line; (ii) the second one is peaking in the red side of this line at 23 450 cm^{-1}. Qualitatively, this spectrum resembles to that measured in our former work on the $Ba(Ar)_n$ system [14]. Following the analysis of the barium data, calcium is thus likely trapped at the surface of the argon cluster. The blue component of the excitation spectrum would be associated with the $4p$ excited orbital pointing towards the cluster (a "$^1\Sigma$" state in a pseudo diatomic picture of the Ca–cluster system). Similarly the red component would correspond to the $4p$ excited orbital parallel to the cluster surface (a "$^1\Pi$" state in the pseudo diatomic picture).

Notice in Figure 2 that the shape of the broad emission due to solvated Ca is the same, regardless of which band is excited. Presumably, this is due a relaxation process that has been documented for the $Ba^*(Ar)_n$ system [29] that is transposed here for calcium. Whatever its initial alignment, parallel or perpendicular to the cluster surface, the excited $4p$ orbital of solvated calcium moves parallel to the cluster surface prior to fluorescence emission and calcium emits from the bottom well of the "Π" potential.

4.3 Absorption spectrum

The simulated absorption spectrum is displayed in Figure 4. It is compared to the experimental excitation spectra in the same figures. The experiment does not provide an absolute photon yield. Hence, a normalization must be chosen. The two experimental spectra have been

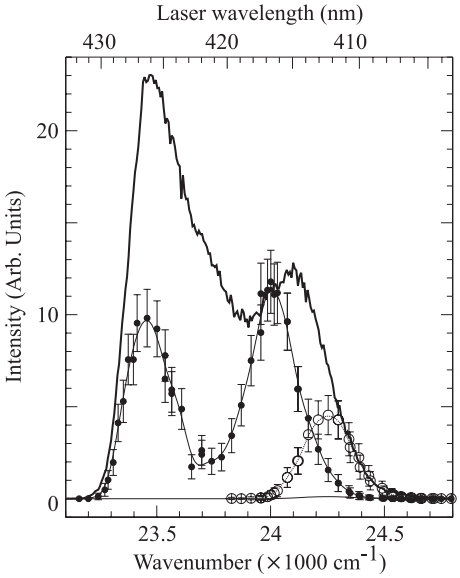

Fig. 4. Simulated absorption spectrum and fluorescence excitation spectrum measured experimentally.

normalized independently with respect to the simulated absorption spectrum. The normalization used is consistent with the fact that the absorption spectrum must overlap the excitation spectra of the calcium fluorescence.

The simulated absorption spectrum consists of two bands in the ratio 2:1, the most intense being the red one. This splitting is similar to that observed in the excitation spectrum of the total calcium fluorescence. It is interpreted above in terms of surface solvation of calcium by comparison with a former work on the $Ba(Ar)_n$ system. This could have been expected when considering that the equilibrium distance of an Ar–Ar pair ($R_e = 7.00a_0$) is much smaller than that of Ca–Ar ($R_e = 9.48a_0$) while the reverse holds for the interaction energies ($D_e = 99$ cm^{-1} for Ar_2, 96 cm^{-1} for CaAr). It has been checked in the simulation directly that Ca remains actually at the surface of the cluster. For this purpose, and to get an idea of the fluctuation of the relative position of calcium and the neighboring argon atoms at $T = 35$ K, Figure 5 shows the radial density of argon atoms about the calcium atom. Both the intensity of the peak at $r = 11a_0$ and the overall decrease of the distribution over a width comparable with the cluster diameter supports the picture of the calcium atom located at the surface. This is further comforted by comparing the present absorption spectrum with the spectra calculated for a calcium atom in bulk argon (periodic boundaries are used in the simulation), or remaining inside a large argon cluster of the same size. The corresponding spectra are plotted in Figure 6.

Now that surface solvation of calcium is confirmed by the simulation, we question the statement of the above subsection regarding the attribution of the two bands observed in Figure 4 to absorption by configurations, respectively parallel to the cluster surface for the red band ("$^1\Pi$" excitation), and perpendicular to the surface for the blue band ("$^1\Sigma$" excitation).

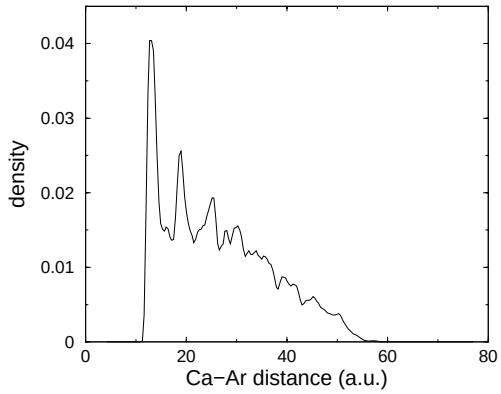

Fig. 5. Radial density of argon atoms around Ca for $CaAr_{308}$ at $T = 35$ K.

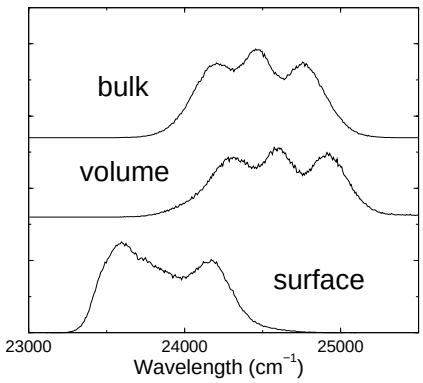

Fig. 6. Comparison of absorption spectra of $CaAr_{308}$, the calcium atom being either in bulk argon, inside (volume) or outside (surface) an argon cluster. The cluster temperature is $T = 35$ K.

With this purpose, we analyze the nature of the absorbing excited states by calculating their overlaps with radial Ψ_Σ and perpendicular Ψ_{Π_x}, Ψ_{Π_y} singlet components. These are defined as

$$\Psi_\Sigma = \frac{1}{\sqrt{2}}\left(a^\dagger_{\sigma\alpha}a_{s\alpha} - a^\dagger_{\sigma\beta}a_{s\beta}\right)\Phi_0, \tag{11}$$

and similar expressions for Ψ_{Π_x} and Ψ_{Π_y}. The σ (resp. π_x, and π_y) orbitals are defined as directed along (resp. perpendicular to) the radial axis between the center of mass of the argon cluster and the calcium atom. For each geometry in the Monte Carlo trajectory and for each excited state m, we calculate the radial and perpendicular weights ρ^m_Σ and ρ^m_Π

$$\begin{aligned}\rho^m_\Sigma &= |\langle\Psi_m|\Psi_\Sigma\rangle|^2,\\ \rho^m_\Pi &= |\langle\Psi_m|\Psi_{\Pi_x}\rangle|^2 + |\langle\Psi_m|\Psi_{\Pi_y}\rangle|^2.\end{aligned} \tag{12}$$

The $(\varepsilon_{0m}, \rho^m_\Sigma)$ couples are represented in a scatter plot in Figure 7. It is clearly seen in this figure that the blue band, near 24 000 cm^{-1}, is correlated with $\rho_\Sigma \approx 1$, whereas the red band correlates with $\rho_\Sigma \approx 0$.

With this in mind, the ratio 2:1 between the two bands could be understood as due to the AIM assumption when calculating transition dipolar moments, and the fact that

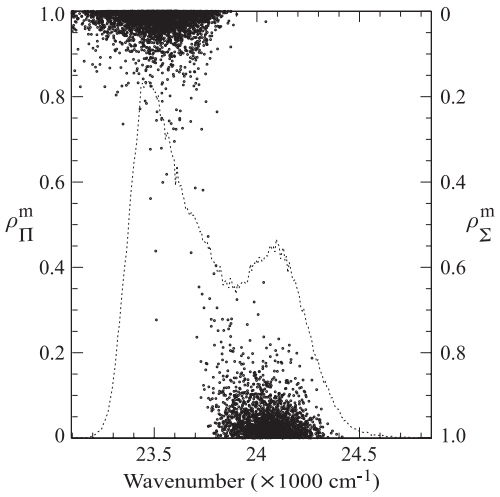

Fig. 7. Radial weights ρ^m_Π (left scale) and ρ^m_Σ (right scale) *versus* transition energy ε_{0m} calculated in $CaAr_{300}$ clusters at $T = 35$ K. The dashed curve recalls the simulated absorption spectrum shown in Figure 4.

the diatomic-like "$^1\Pi$" state contributes twice to the integrated intensity ("$^1\Pi_x$" and "$^1\Pi_y$"). It should be clear that the calculated spectra result from the summation over numerous microscopic configurations, among which very few actually exhibit a perfect x, y degeneracy, and are moreover averaged over several sizes.

Let us examine Figure 4 in more detail. The agreement between the simulated absorption spectrum and the experimental excitation spectra is quantitative concerning the location of the set of two bands. In particular, the red wing of the absorption spectrum matches approximately that of the experimental spectrum for the excitation of the total fluorescence. Similarly, the blue wing of the simulated absorption spectrum matches that of the other experimental spectrum where calcium emits as a free atom. Moreover, the splitting of the simulated absorption spectrum into two bands matches approximately that found experimentally on the excitation spectrum of the total calcium fluorescence.

The simulated blue band peaks and extends towards higher energies by an extra $\sim$ 100 cm^{-1}. Obviously, it difficult for theory to achieve an absolute accuracy of this magnitude, especially for clusters with such sizes. Causes may be found in assumptions inherent to the DIM model. This includes the diatomic inputs used in its parameterization. The CaAr potential curves, determined in a recent work [15], turns out to approach the spectroscopic accuracy: for the ground molecular state $4s^2\ ^1\Sigma^+$, the quantities ω_e, $\omega_e x_e$ and D_0 have respectively the values 18.3 cm^{-1}, 1.77 cm^{-1} and 87.0 cm^{-1} when deduced from the calculated potential curve, *versus* 18 cm^{-1}, 1.9 cm^{-1} and 53 ± 10 cm^{-1} in the experiment [30]; however, reference [15] recommends a value of 72.5 cm^{-1} for D_0 which is closer to the theoretical value of 87.0 cm^{-1} ($D_e = 96$ cm^{-1}) used in the present calculation; for the excited $4s4p\ ^1\Pi$ molecular state, the same quantities are calculated to be 22.79 cm^{-1}, 1.69 cm^{-1} and 146.3 cm^{-1}, and are found to be 22 cm^{-1}, 1 cm^{-1} and 123 ± 10 cm^{-1} experimentally [30]. Finally, another source of error is obviously the different cluster sizes involved in the simulation and in the experiment. It is difficult for simulation to estimate the corresponding error. Nevertheless, finite size effects between 300 and 2 000 atoms are expected to be reasonably small at 35 K. It is also difficult to account precisely for the broad size distribution in the experiment. Despite the above errors, we notice that the excitation spectra of the calcium fluorescence falls within the theoretical limits. This agreement reflects the overall relevance of the present DIM model.

More interesting is the comparison between the shape of the simulated absorption spectrum and the experimental excitation spectrum of the total fluorescence. The absorption spectrum has a broader red band than the excitation spectrum, and a maximum of the blue band that is shifted even more to the blue side. Moreover, the intensity ratio between the red and blue bands is about 2:1 in the absorption spectrum and about 0.8:1 in the excitation spectrum.

Of course, these differences could be attributed to inaccuracies in the potentials, but we just have seen that it is unlikely. They could also be due to the DIM approximation falling apart since it does not account fully for n-body effects, or to the inadequacy of the AIM assumption when calculating transition dipole moments. Work is in progress to directly calculate energy levels, and especially wavefunctions of the $Ca(Ar)_n$ system beyond the AIM and DIM assumptions. This may result into oscillator strengths towards the "$^1\Pi$" and "$^1\Sigma$" states that differ from the 2:1 ratio mentioned above. Indeed, the presence of several argon atoms at the surface may induce non additive effects as well as distortions of the wavefunctions, not included in the DIM model.

Nevertheless, in view of the qualitative large difference between the calculated absorption spectrum and the excitation spectrum of the total calcium fluorescence, other processes must be invoked also, such as collisional quenching, a process associated with the excited state dynamics calcium that is considered hereafter.

Figure 1 reveals that the $^3\Sigma^+$ curve correlating with the Ca($4s3d\ ^3$D)+Ar asymptote crosses the $^1\Pi$ curve correlating with Ca($4s4p\ ^1$P)+Ar. From reference [15] we know that the crossing is located about 700 cm^{-1} above the well of the $^1\Pi$ curve. In gas phase collisions between Ca($4s4p\ ^1$P) and argon, this crossing is responsible for the quenching of the calcium excitation towards Ca($4s3d\ ^3$D) [31]. In clusters, the location of the corresponding hypersurface are tedious to predict.

Coming back to the cluster environment and considering the pseudo-diatomic picture of the Ca-cluster system, an equivalent coupling can certainly be anticipated between the "$^1\Pi$" curve correlating to Ca($4s4p\ ^1$P) and the "$^3\Sigma$" curve correlating to Ca($4s3d\ ^3$D). The "$^3\Sigma^+$" curve is certainly more repulsive in the cluster environment than its equivalent in the Ca–Ar pair. Hence, excitation along the "$^1\Pi$" curve by several hundred wavenumbers above the well bottom of the curve might result into energy

transfer towards the dark Ca($4s3d$ ^{3}D) state. The coupling that is responsible for that involves an interconfigurational spin-orbit mixing, which is certainly very small. Therefore, it weakly affects the nature of the absorbing wavefunctions as assumed in the DIM model, hence the absorption spectra. In contrast it may show up in the excitation spectrum of the calcium total fluorescence simply because calcium stays a long time on the cluster before emitting (remember that most of the emission originates from calcium that remains trapped on the cluster) and may experience the coupling with the "$^3\Sigma^+$" curve again and again. The role of configurations related with the ^{1}D asymptote may also play a role.

5 Conclusion

The present work is a combined theoretical and experimental approach documenting the interaction of a single calcium atom with a large argon cluster, the calcium atom being electronically excited in the vicinity of the resonant state $4s4p$ ^{1}P$_1$. Three different spectroscopies have been used for this purpose: emission spectroscopy, excitation spectroscopy of both dispersed and total fluorescence, and absorption spectroscopy. The first two spectroscopic investigations are experimental. They concern calcium deposited on argon clusters of average size 2 000. The corresponding experiments have been conducted in a beam, the emission and excitation spectra have been obtained using the Laser Induced Fluorescence technique. The third investigation concerns the numerical simulation of the absorption spectrum of calcium when deposited on clusters of average size 300. The simulation associates Diatomics-In-Molecules potentials to describe the excited calcium-cluster interaction and a Monte Carlo calculation to sample geometries of the ground state Ca-cluster system. High quality potential curves have been used to describe the ground state $4s^2$ and the excited state $4s4p$ configurations of the Ca–Ar pair that are to be used in the MC calculation and in the DIM model.

The results and the comparison between the experiment and the simulation lead to the following picture. Calcium is deposited at the surface of the argon cluster. This results into the splitting of the fluorescence excitation spectrum of calcium into two bands. One is assigned to the excitation of the $4p$ orbital of calcium perpendicular to the cluster surface (excitation towards a "$^1\Sigma$" curve in a pseudo-diatomic picture of the Ca-cluster system). The other band corresponds to excitation of "$^1\Pi$" curve, with the $4p$ orbital parallel to the cluster surface.

Excitation towards the "$^1\Sigma$" curve can result into the ejection of calcium out of the cluster, but this channel is minor. Otherwise, calcium emits light after relaxation of the $4p$ orbital parallel to the cluster surface. Excitation towards the "$^1\Pi$" curve never results into ejection of electronically excited calcium for energetic reasons.

Interestingly, the calculated absorption spectrum fall in the same spectral range as the experimental spectra for exciting the calcium fluorescence. In particular, the calculated "$^1\Pi$" and "$^1\Sigma$" bands have approximately the same location and width as the corresponding bands in the experimental spectrum for exciting the total fluorescence of calcium. However, These bands are in the ratio 0.8:1 in the experimental spectrum whereas they are in the ratio 2:1 in the numerical simulation of the absorption spectrum, a phenomenon that might be attributed to a non adiabatic coupling between the "$^1\Pi$" potential curve and a "$^3\Sigma^+$" curve that correlates with the Ca($4s3d$ ^{3}D)–Ar$_n$ asymptote. Of course an alternative interpretation would be inadequacies in the assumptions of the DIM and AIM calculations. We do not consider that the latter could account solely for the observed difference between the absorption spectrum and the excitation spectrum of the total calcium fluorescence. Hence the present work seems to focus the attention on a non adiabatic singlet-to-triplet energy transfer that is induced in the calcium atom by the fluctuating interaction with an argon cluster at non zero temperature.

To our knowledge, such a process involving the configuration change of a chromophore coupled to a thermostat has never been investigated yet, theoretically. This motivates to further develop the present theoretical approach in the following directions. Firstly, the transition moments should be checked on the Ca–Ar diatomics and on small CaAr$_n$ clusters, for instance by using a pseudopotential formalism similar to the studies on alkali-rare gases systems [32–34], but involving here two active electrons. A lot of the information comes indeed from the comparison between the ratio of the the "$^1\Sigma$" and "$^1\Pi$" bands, hence it is important to predict this ratio without ambiguity. Secondly, the DIM Hamiltonian could be upgraded by including the $4s3d$ configurations. This would require preliminary diabatization to be achieved on the diatomic states. This step is of considerable importance since it will ultimately allow for the desired investigation of the relaxation dynamics of the excited states in the environment of the argon cluster.

Partial support from the CNRS is acknowledged through the Groupement de Recherche "agrégats, dynamique et réactivité".

References

1. C. Gée, M.A. Gaveau, J.M. Mestdagh, M.A. Osborne, O. Sublemontier, J.P. Visticot, J. Phys. Chem. **100**, 13421 (1996)
2. J.M. Mestdagh, M.A. Gaveau, C. Gée, O. Sublemontier, J.P. Visticot, Int. Rev. Phys. Chem. **16**, 215 (1997)
3. M.A. Gaveau, C. Gée, J.M. Mestdagh, J.P. Visticot, Comm. At. Mol. Phys. **34**, 241 (1999)
4. X. Biquard, O. Sublemontier, J. Berlande, M.A. Gaveau, J.M. Mestdagh, B. Schilling, J.P. Visticot, J. Chim. Phys. **92**, 264 (1995)
5. R. Baumfalk, N.H. Nahler, U. Buck, M.Y. Niv, R.B. Gerber, J. Chem. Phys. **113**, 329 (2000)
6. P. Slavicek, P. Zdanska, P. Jungwirth, R. Baumfalk, U. Buck, J. Phys. Chem. A **104**, 7793 (2000)

7. R. Baumfalk, N.H. Nahler, U. Buck, Faraday Discuss. **118**, 247 (2001)
8. M.A. Gaveau, M. Briant, P.R. Fournier, J.M. Mestdagh, J.P. Visticot, Phys. Chem. Chem. Phys. **2**, 831 (2000)
9. E. Lugovoj, J.P. Toennies, A. Vilesov, J. Chem. Phys. **112**, 8217 (2000)
10. Z. Liu, H. Gómez, D.M. Neumark, Faraday Discuss. **118**, 221 (2001)
11. M. Briant, M.A. Gaveau, P.R. Fournier, J.M. Mestdagh, J.P. Visticot, B. Soep, Faraday Discuss. **118**, 209 (2001)
12. F. Stienkemeier, F. Meier, H.O. Lutz, J. Chem. Phys. **107**, 10816 (1997)
13. J.P. Visticot, J. Berlande, J. Cuvellier, A. Lallement, J.M. Mestdagh, P. Meynadier, P. de Pujo, O. Sublemontier, Chem. Phys. Lett. **191**, 107 (1992)
14. J.P. Visticot, P. de Pujo, J.M. Mestdagh, A. Lallement, J. Berlande, O. Sublemontier, P. Meynadier, J. Cuvellier, J. Chem. Phys. **100**, 158 (1994)
15. F. Spiegelman, L. Maron, W.H. Breckenridge, J.-M. Mestdagh, J.-P. Visticot, J. Chem. Phys. (accepted, 2002)
16. C. Gée, M.A. Gaveau, O. Sublemontier, J.M. Mestdagh, J.P. Visticot, J. Chem. Phys. **107**, 4194 (1997)
17. M. Briant, M.A. Gaveau, J.M. Mestdagh, J.P. Visticot, J. Chem. Phys. **112**, 1744 (2000)
18. R. Campargue, J. Phys. Chem. **88**, 4466 (1984)
19. T.E. Gough, M. Mengel, P.A. Rowntree, G. Scoles, J. Chem. Phys. **83**, 4958 (1985)
20. S. Goyal, D.L. Schutt, G. Scoles, Chem. Phys. Lett. **196**, 123 (1992)
21. L.C. Balling, J.J. Wright, J. Chem. Phys. **79**, 2941 (1983)
22. J.A. Boatz, M.E. Fajardo, J. Chem. Phys. **101**, 3472 (1994)
23. O. Roncero, J.A. Beswick, N. Halberstadt, B. Soep, NATO ASI Ser. B **227**, 471 (1990)
24. J.S. Cohen, B.S. Schneider, J. Chem. Phys. **61**, 3230 (1974)
25. C.E. Moore, *Atomic Energy Levels*, Circular 467, Vol I, NBS, US Dept. of Commerce, 1949
26. M. Grigorov, F. Spiegelman, Surf. Rev. Lett. **3**, 211 (1996)
27. J. Farges, M.F. de Feraudy, B. Raoult, G. Torchet, Surf. Sci. **106**, 95 (1981)
28. B. Schilling, M.A. Gaveau, O. Sublemontier, J.M. Mestdagh, J.P. Visticot, X. Biquard, J. Berlande, J. Chem. Phys. **101**, 5772 (1994)
29. A.I. Krylov, R. Benny Gerber, M.A. Gaveau, J.M. Mestdagh, B. Schilling, J.P. Visticot, J. Chem. Phys. **104**, 3651 (1996)
30. A. Kowalski, D.J. Funk, W.H. Breckenridge, Chem. Phys. Lett. **132**, 263 (1986)
31. W.H. Breckenridge, C.N. Merrow, J. Chem. Phys. **88**, 2320 (1988)
32. C. Tsoo, D.A. Estrin, S.J. Singer, J. Chem. Phys. **93**, 7187 (1990)
33. C. Tsoo, D.A. Estrin, S.J. Singer, J. Chem. Phys. **96**, 7977 (1992)
34. G. Martyna, C. Cheng, M.L. Klein, J. Chem. Phys. **95**, 1318 (1991)